Supplementary Information for

A Universal Magnetic Alignment Strategy for Composite Solid-state electrolytes with Vertically Aligned High-Ionic-Conductivity Pathways

Hui Ding[a], Wen He[a], Haoqing Tian[a], Shuo Liu[a], Wensheng Yang*[a,b]

[a]State Key Laboratory of Chemical Resource Engineering, Beijing University of Chemical Technology, Beijing 100029, P. R. China

[b]Quzhou Institute for Innovation in Resource Chemical Engineering, No. 78, Jiuhuabei Avenue, Quzhou City, Zhejiang Province 324000, P. R. China

* Corresponding author. E-mail: yangws@mail.buct.edu.cn (Wensheng Yang)

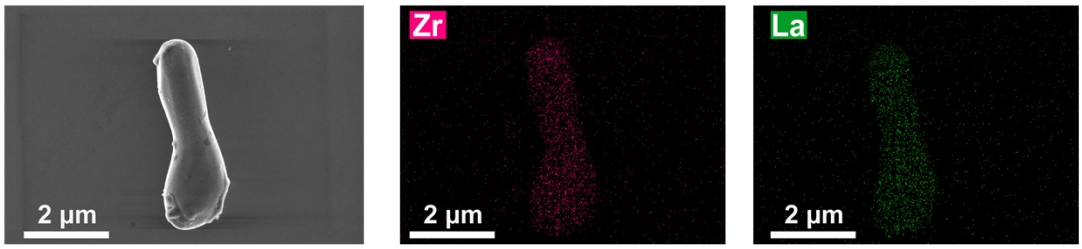

Fig. S1. SEM image and EDS elemental mappings of Zr and La for an individual LLZO.

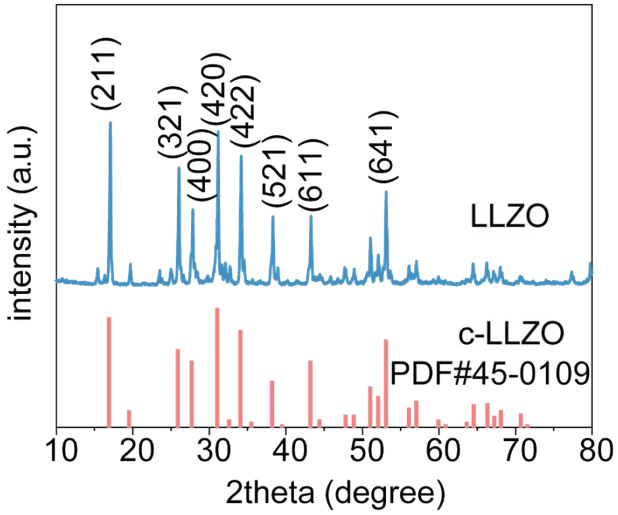

Fig. S2. X-Ray Diffraction (XRD) patterns of the cubic-$Li_7La_3Zr_2O_{12}$ (LLZO) nanoparticles. The XRD pattern of LLZO shows characteristic peaks that match well with the standard card for cubic LLZO. The measurement was performed from 10° to 80° (2θ) at a scanning rate of $10°\cdot min^{-1}$.

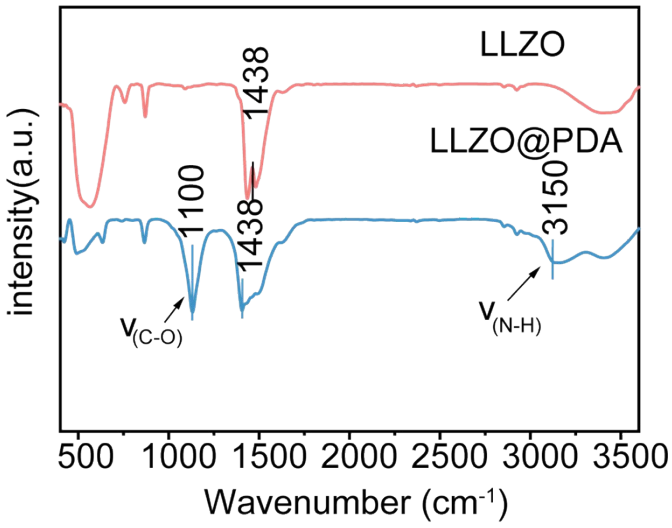

Fig. S3. Fourier Transform infrared spectroscopy (FT-IR) of LLZO without and with PDA coating. The FT-IR spectrum of coated LLZO shows characteristic peaks of PDA at 1100 cm^{-1} (C–O) and 3150 cm^{-1} (N–H).

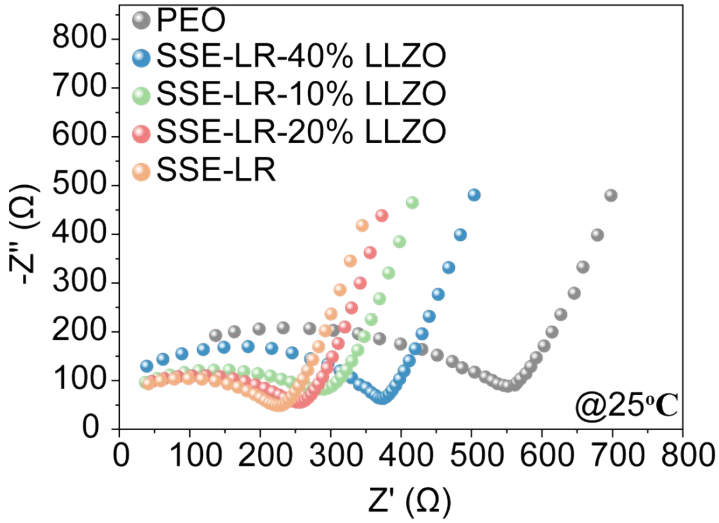

Fig. S4. Nyquist plots for samples containing 10–40 wt.% LLZO@PDA (relative to the PEO matrix). The sample with 30 wt.% LLZO@PDA is denoted as SSE-LR. The ionic conductivities of the LLZO@PDA/PEO composite solid-state electrolytes with LLZO@PDA contents ranging from 10 to 40 wt.% were calculated using the formula $\sigma = L/(R \cdot S)$ (R is impedance value; L is membrane thickness; S is membrane area).

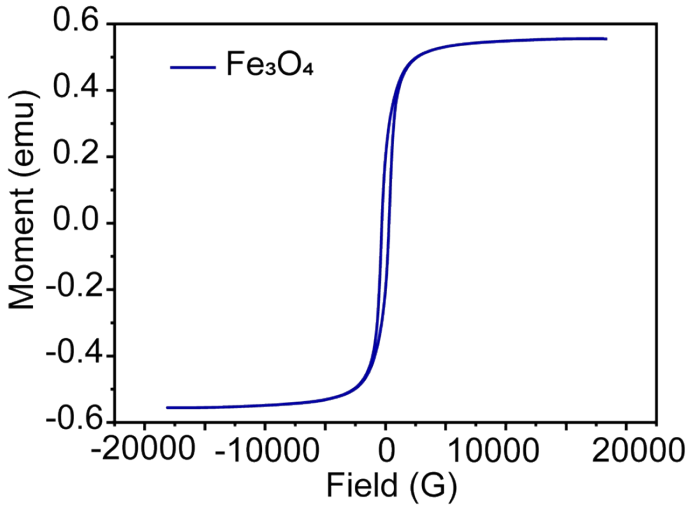

Fig. S5. Vibrating Sample Magnetometer curve of the Fe_3O_4 nanorods. The saturation magnetization (M_s) was calculated to be 92.5 emu·g^{-1} from the measured magnetic moment and a 6 mg sample mass.

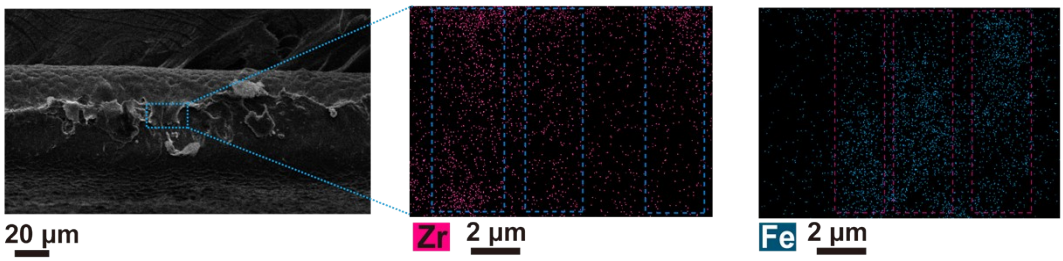

Fig. S6. Cross-sectional SEM and elemental mappings of the SSEM-LV membrane after being kept at 60 °C for 24 h.

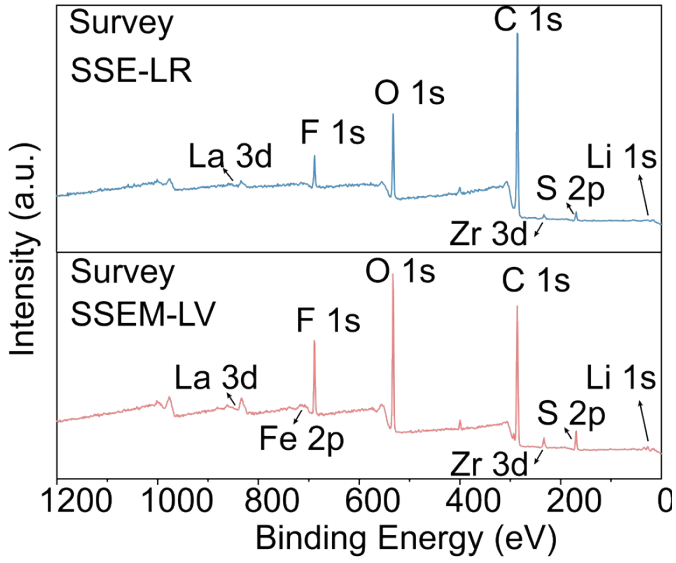

Fig. S7. XPS survey of SSE-LR and SSEM-LV.

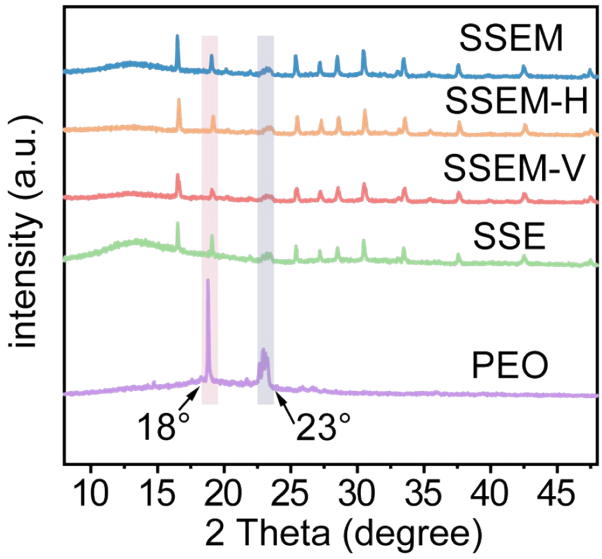

Fig. S8. XRD pattern of SSEM-LV, SSEM-LR, SSEM-LH, SSE-LR and PEO. The XRD patterns were collected from 10° to 80° (2θ) at a scan rate of 10°·min^{-1}. The decreased intensity of the characteristic peaks compared to pure PEO suggests that the crystallization of the PEO polymer matrix was suppressed by the incorporation of LLZO@PDA and Fe_3O_4.

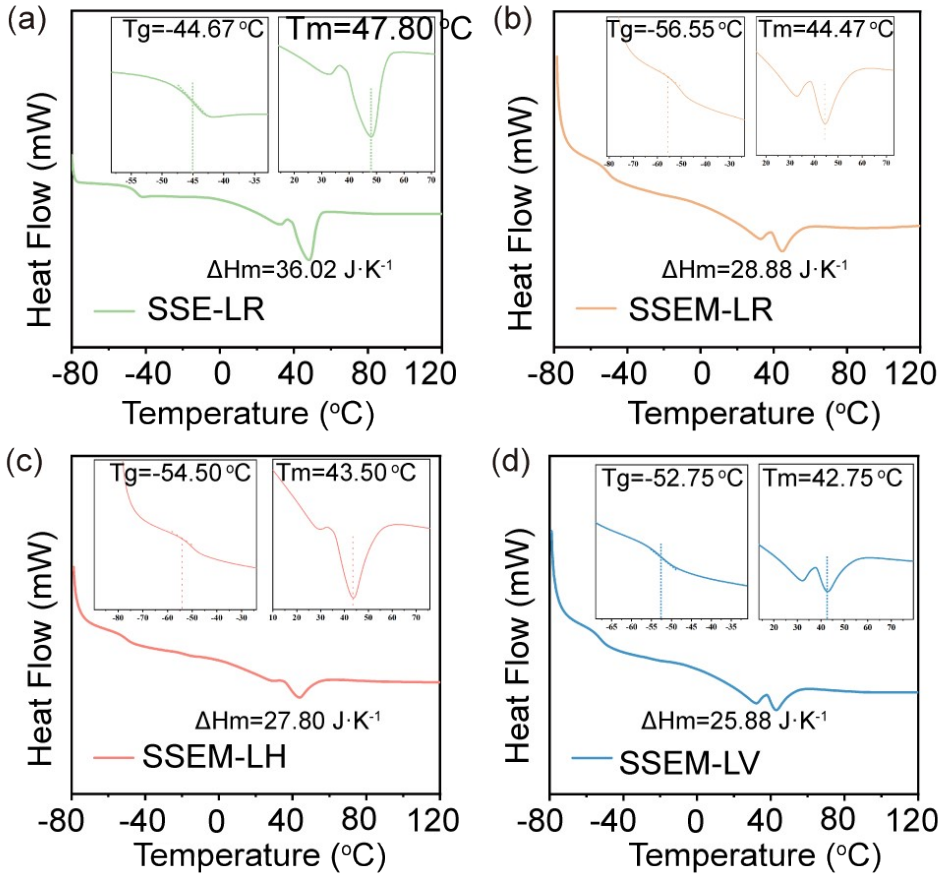

Fig. S9. Differential Scanning Calorimetry (DSC) curves of (a) SSE-LR, (b) SSEM-LR, (c) SSEM-LH and (d) SSEM-LV. DSC was employed to characterize the phase transition behavior of each electrolyte. The crystallinity (χc) of the four electrolytes was calculated according to $\chi_c = \Delta H_m / (\Delta H_{PEO} * f_{PEO}) * 100\%$, where ΔH_m is the melting enthalpy of the membrane, ΔH_{PEO} is the melting enthalpy of fully crystalline PEO, which is 196.4 $J \cdot g^{-1}$, and f_{PEO} is the weight fraction of PEO in the electrolyte sample (Sustainable Energy & Fuels, 2023, 7, 1645-1655).

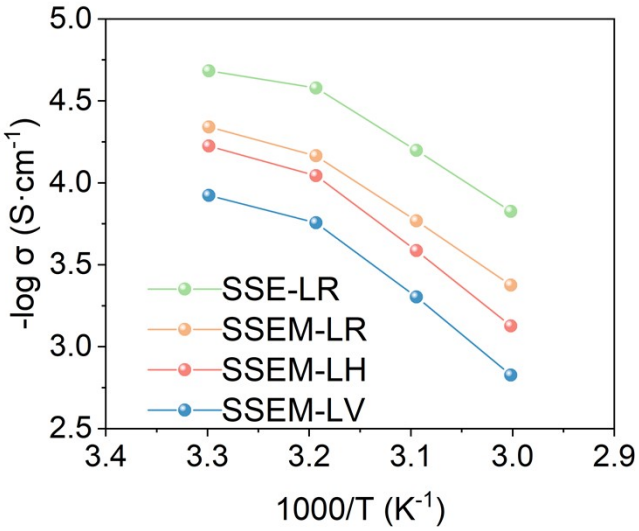

Fig. S10. Arrhenius plots of ionic conductivity for SSE-LR, SSEM-LR, SSEM-LV and SSEM-LH. SSEM-LV exhibits the highest ionic conductivity from 30 to 60 °C; For instance, at 60 °C, the ionic conductivities of SSEM-LV, SSEM-LR, SSEM-LH and SSE-LR are 12.9×10^{-4} S·cm^{-1}, 6.6×10^{-4} S·cm^{-1}, 4.6×10^{-4} S·cm^{-1}, 1.0×10^{-4} S·cm^{-1}, respectively.

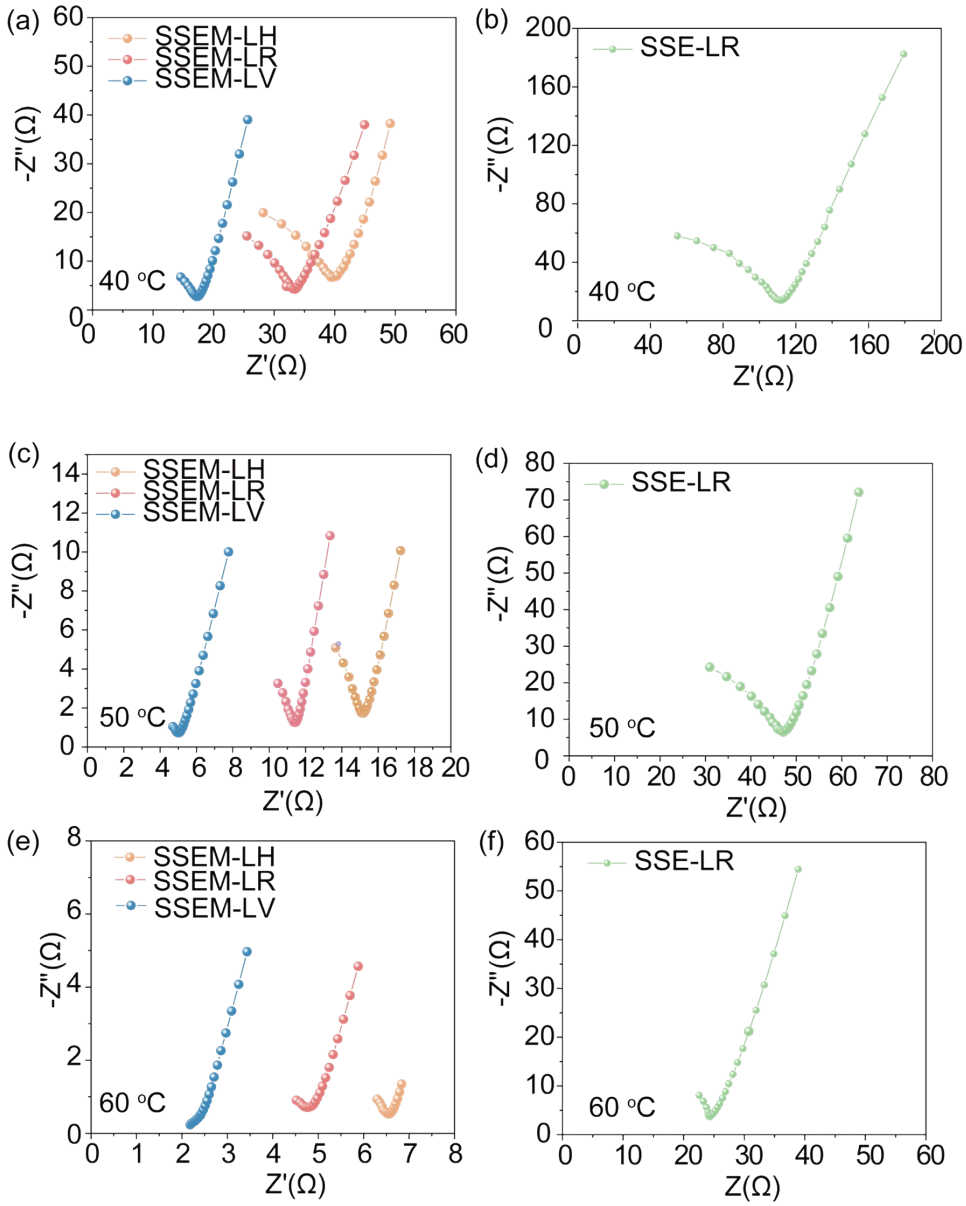

Fig. S11. Nyquist plots of SSE-LR, SSEM-LR, SSEM-LV and SSEM-LH at 40, 50, and 60 °C.

Table S1. Ionic conductivity ($\times 10^{-4}$ S·cm^{-1}) of SSE-LR, SSEM-LR, SSEM-LV and SSEM-LH at 30, 40, 50 and 60 °C

Sample	30 °C	40 °C	50 °C	60 °C
SSEM-LV	1.20	1.70	7.40	12.9
SSEM-LR	0.55	0.90	1.80	4.60
SSEM-LH	0.46	0.74	2.60	6.60
SSE-LR	0.21	0.26	0.64	1.00

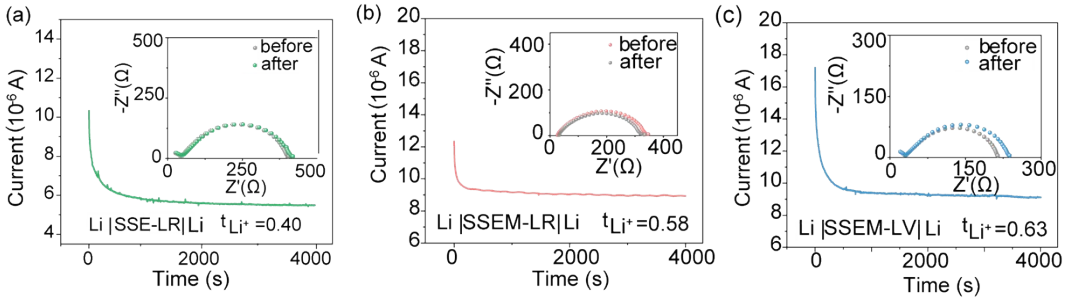

Fig. S12. I-t curves of SSE-LR, SSEM-LR and SSEM-LV (inset: impedance plots before and after the I-t test).

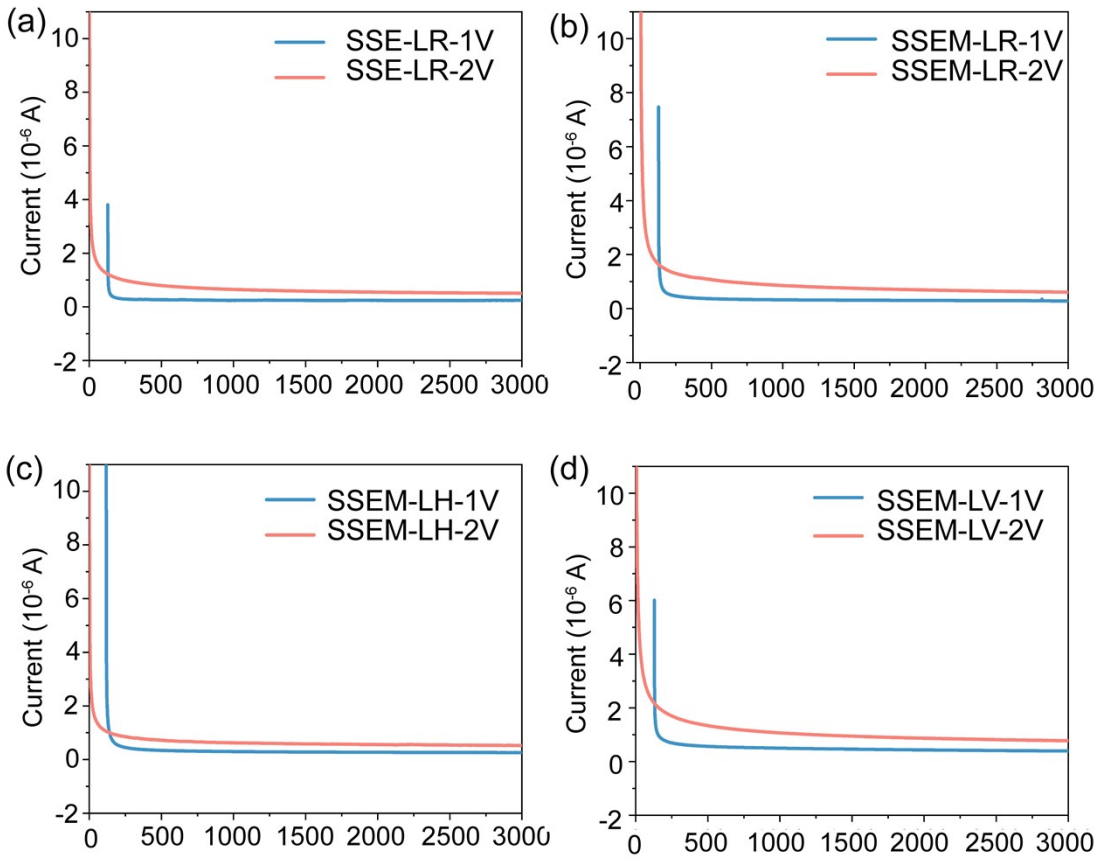

Fig. S13. Chronoamperometry (i-t) curves of (a) SSE-LR (b) SSEM-LR (c) SSEM-LH and (d) SSEM-LV measured at 60℃. The electronic conductivities of the composite electrolytes were evaluated via DC polarization measurements using an ion-blocking configuration (SS|electrolyte|SS) (Nature Energy, 2019, 4, 187–196). Upon the application of a constant DC voltage, the current initially decayed rapidly due to the ion-blocking effect of the stainless steel electrodes and eventually stabilized. This steady-state current is attributed solely to electron migration. Calculated from the steady-state currents, the electronic conductivities of SSE-LR, SSEM-LR, SSEM-LH, and SSEM-LV are 7.43×10^{-10} S·cm^{-1}, 8.12×10^{-10} S·cm^{-1}, 7.77×10^{-10} S·cm^{-1}, 11.2×10^{-10} S·cm^{-1}, respectively.

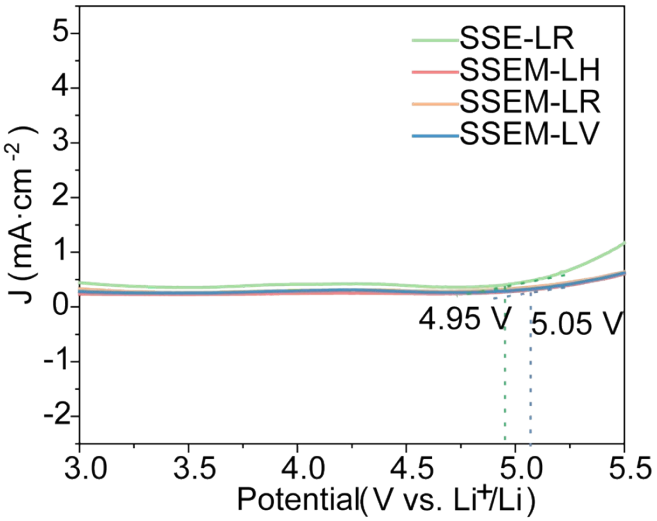

Fig. S14. Linear sweep voltammetry (LSV) curves of SSEM-LV, SSEM-LR, SSEM-LH and SSE-LR, measured using an SS||Li cell at a scan rate of 5 $mV \cdot s^{-1}$ over a potential range of 3.0–5.5 V (vs. Li^+/Li).

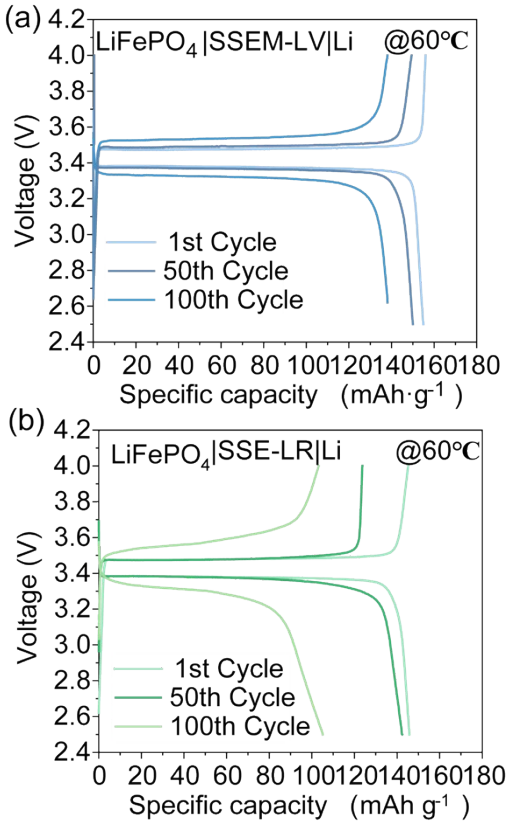

Fig. S15. Charge and discharge curves of $LiFePO_4$||Li cells with (a) SSEM-LV and (b) SSE-LR at selected cycle numbers. Tests were performed at 60 °C and 0.1 C over a voltage range of 2.5-4.0 V (vs. Li^+/Li).

Table S2 Comparison of electrochemical performances and loading of LFP in literatures

Ionic conductivity (10^{-4} S·cm^{-1})	Lithium anode stability	LFP-Li cell Specific capacity	Loading of LFP (mg·cm^{-2})	Journals
0.48 (30 °C)	0.1mA·cm^{-2} 480h	LFP, 0.1C 140.4 mAh·g^{-1}	---	Journal of Colloid and Interface Science 565 (2020) 110–118
4.4 (60 °C)	0.05mA·cm^{-2} 600h	LFP, 4C, 121 mAh·g^{-1}	1.0	Rare Met. 42, 875–884 (2023)
2.1 (60 °C)	0.1 mA·cm^{-2} 350h	LFP, 0.1C 121 mAh·g^{-1}	3.2	Journal of Energy Chemistry 70 (2022) 363–372
1.15 (30 °C)	0.2 mA·cm^{-2} 400h	LFP, 0.2C 147 mAh·g^{-1}	----	J. Mater. Chem. A, 2019,7, 16425-16436
0.85 (60 °C)	0.1 mA·cm^{-2} 800h	LFP, 0.2C 120 mAh·g^{-1}	1.0	Chemical Engineering Journal 524 (2025) 169042
0.43 (30 °C)	0.05mA·cm^{-2} 1000h	LFP, 0.1C 150 mAh·g^{-1}	1.1	Chemical Engineering Journal 429 (2022) 132343
0.31 (30 °C)	0.2 mA·cm^{-2} 280h	---	----	Energy Storage Materials 28 (2020) 293–299
1.39 (30 °C)	0.1 mA·cm-2 120h	LFP, 0.1C 140 mAh·g^{-1}	2.2	Adv. Sci. 2018, 5, 1700996
0.32 (30 °C)	----	LFP, 0.1C 125 mAh·g^{-1}	-----	Electrochimica Acta 389 (2021) 138747
1.20 (30 °C) 12.9 (60 °C)	**0.05mA·cm^{-2} 700h**	**LFP, 0.1C 155.9 mAh·g^{-1}**	**3.57**	**This work**

As detailed in **Table S2**, SSEM-LV demonstrates the following specific parameters: i) Ionic conductivities of 1.2×10^{-4} S·cm^{-1} at 30 °C and 12.9×10^{-4} S·cm^{-1} at 60 °C. The value at 60 °C is higher than those of the other references listed in the table. ii) The LFP||Li cell delivers a specific capacity of 155.9 mAh·g^{-1} at 0.1C, which is the highest

value among the compared references. iii) The LFP loading in our work is 3.57 $mg \cdot cm^{-2}$, which is higher than the referenced values. iv) SSEM-LV exhibits a stable cycle life of 700 h at 0.05 $mA \cdot cm^{-2}$, which is comparable to that reported in the existing literature.